The first larval age and growth curve for bluefin tuna (*Thunnus thynnus*) from the Gulf of Mexico: comparisons to the Straits of Florida, and the Balearic Sea (Mediterranean)

Estrella Malca[1,2], Barbara Muhling[3,4], James Franks[5], Alberto García[6], Jason Tilley[5], Trika Gerard[2], Walter Ingram Jr.[2], John T. Lamkin[2]

[1]Cooperative Institute for Marine and Atmospheric Studies, Rosenstiel School of Marine and Atmospheric Science, University of Miami, 4600 Rickenbacker Causeway, Miami FL 33149, USA. Estrella.Malca@noaa.gov

[2]Southeast Fisheries Science Center, National Marine Fisheries Service, National Oceanic and Atmospheric Administration (NOAA), 75 Virginia Beach Drive, Miami FL, USA. Estrella.Malca@noaa.gov, Trika.Gerard@noaa.gov, John.Lamkin@noaa.gov, Walter.Ingram@noaa.gov

[3]Princeton University Program in Atmospheric and Oceanic Science, Forrestal Campus/Sayre Hall, Princeton, NJ, USA. Barbara.Muhling@noaa.gov

[4]NOAA Geophysical Fluid Dynamics Laboratory, 201 Forrestal Road, Princeton, New Jersey, USA. Barbara.Muhling@noaa.gov

[5]The University of Southern Mississippi, Gulf Coast Research Laboratory, Center for Fisheries Research and Development, 703 East Beach Drive, Ocean Springs, MS, USA. Jim.Franks@usm.edu, jason.tilley@usm.edu

[6]Centro Oceanográfico de Málaga, Instituto Español de Oceanografía, 29640 Fuengirola, Málaga, Spain. Agarcia@ma.ieo.es

Corresponding author: Estrella Malca

Highlights

- We present the first larval BFT growth curve derived from the Western spawning grounds
- Larval bluefin tuna growth for Gulf of Mexico larvae was significantly faster when compared to previous studies
- Daily growth trajectories diverged with ontogeny for Gulf of Mexico bluefin tuna otoliths

Abstract

Atlantic bluefin tuna (*Thunnus thynnus*) undertake extensive migrations throughout the North Atlantic Ocean, but spawn primarily in the Gulf of Mexico (GOM) and the Mediterranean Sea. Little is known about larval bluefin tuna (BFT) dynamics and growth despite numerous surveys conducted in the GOM. In this study, we describe age-length relationships for larval BFT using otolith increment analysis and compare somatic daily growth as revealed by individual increment widths from the GOM. Otoliths (sagittae) were aged from pre and post flexion larvae collected during multiple spring spawning seasons in 2000 to 2012 (259 larvae, 2.1–10.9 mm body length, 0–15 daily increments). For the first time, larval growth from the GOM is compared to historical larval collections in the neighboring Straits of Florida and in the Balearic Sea. Our results indicate that growth for GOM larvae is significantly faster than reported from previous studies, indicating different growth strategies during the larval stages for the two spawning grounds. This new growth curve will be incorporated into the calculations of the annual larval index used in the management of this overfished species. Growth and its variability, are important drivers, integral in studies of larval ecology dynamics for BFT.

Keywords: Atlantic bluefin tuna, larval growth, microstructure analysis,
otolith biometrics, Thunnus thynnus

1. Introduction

Atlantic bluefin tuna, *Thunnus thynnus* (BFT) are the largest and among the most valuable overfished scombrids in the North Atlantic Ocean (Rooker et al. 2007, Restrepo et al. 2010, Anonymous 2014). Numerous BFT studies have been conducted to inform management decisions and has advanced our understanding of various aspects of their ecology (Fromentin & Powers 2005; Secor et al. 2008; Rooker et al. 2008). Larval studies have focused on distribution and habitat associations (Alemany et al. 2010; Muhling et al. 2010, 2011, 2013), feeding ecology (Reglero et al. 2014, Yúfera et al. 2014, Tilley et al. 2016), larval condition in the Balearic Sea (García et al. 2006), and most recently, comparative trophic ecology between spawning grounds (Laiz-Carrión et al. 2015). Faster larval growth is generally a good indicator of larval survival, but hatchery and field experiments indicate this relationship is species-specific (Hare & Cowen 1997, Tanaka et al. 2006, Fiksen et al. 2007, García et al. 2013). However, the contribution of larval BFT growth dynamics remains largely unexplored, despite the need to improve our understanding of early life history and its unidentified links to recruitment.

Spawning of BFT is regionally distinct, with nearly all of the western stock spawning in the GOM (Richards 1976) and the eastern stock spawning principally in the Mediterranean Sea (Fromentin & Powers 2005) (Figure 1). Strong repeat homing behavior drives separation of the stocks (Block et al. 2005, Rooker et al. 2008, Wilson et al. 2015). Spawning occurs in the GOM between April and June (Richards 1976, Scott et al. 1993, Block et al. 2005, Muhling et al. 2013) and takes place mostly in offshore nutrient-poor waters, rather than productive habitats found along the continental shelf (Muhling et al. 2010). Minor spawning events also been recorded along the Gulf Stream, near the Slope Sea, in the Bahamas and in the Mexican Caribbean (McGowan & Richards 1989, Muhling et al. 2011, Lamkin et al. 2014, Richardson et al. 2016). Larvae hatched

in the US Exclusive Economic Zone (EEZ) of the GOM have been sampled annually since 1977 during fisheries-independent plankton surveys carried out by the National Marine Fisheries Service's Southeast Area Monitoring and Assessment Program (SEAMAP) (Lyczkowski-Shultz et al. 2013). Larval abundances from SEAMAP surveys provide yearly estimates of adult spawning biomass by using modeled abundances of day-one larvae derived from larval length distributions (Scott et al. 1993, Ingram et al. 2010).

Otoliths are routinely used to age fishes and generate growth curves that contribute to fisheries stock assessments (Ingram et al. 2010), ecological studies (Hare & Cowen 1997) and to approximate spawning times (Richardson et al. 2016). Daily increments are bipartite structures composed of a transparent layer (L-zone) and a darker but often-wider layer (D-zone) when viewed with transmitted light (Campana & Jones 1992; Secor et al. 1995). Previously, otoliths of larval BFT were aged from specimens collected in the Straits of Florida (SOF) (Brothers et al. 1983) and the Balearic Sea in the Western Mediterranean (García et al. 2006, 2013). Age validation studies have not been conducted for larval BFT; however, Itoh et al. (2000) confirmed daily periodicity of increment formation for Pacific bluefin tuna (*Thunnus orientalis*) from 4 to 71 days. The larval growth curve used in the current management plan for this species is based upon samples collected by Brothers et al. (1983) in the SOF at the edge of the Gulf Stream from 19 May – 2 June 1981 and has not been updated since. To date, larval BFT collected from the primary spawning grounds in the GOM have not been aged.

Complementary to generating growth curves, comparing otolith biometrics can disentangle daily variability within and among larval cohorts as it relates to larval ecosystem dynamics (Sponaugle 2010). Otolith radius (OR) measurements have been utilized to compare cohorts (Quintanilla et al. 2015), while the variability of daily increment widths (IW) has been used as an

indicator of somatic growth (Brothers & McFarland 1981, Shulzitski et al. 2012, Zenteno et al. 2014). Recruitment of BFT exhibits large interannual variability, the drivers of which remain unresolved. Otolith biometrics can facilitate a better understanding of biotic and abiotic drivers that play a key role in the development of credible predictive recruitment models for BFT that ultimately contribute to stock assessment models.

This study replaces the existing BFT larval growth curve by ageing otoliths from larvae collected from the GOM and compares their age at length estimates with those reported for BFT larvae from the SOF (Brothers et al. 1983) and the Balearic Sea (García et al. 2013).

2. Material and methods

2.1. Sample collections

Collections of BFT larvae for this study comprise two separate sampling efforts conducted in the GOM from 2000 to 2012 during the adult spawning seasons. In the first effort, larvae were collected from 2000 to 2010 by the University of Southern Mississippi Gulf Coast Research Laboratory (GCRL dataset henceforth) in a sampling area bounded by longitudes 85.7926° to 89.7498° W and latitudes 24.2703° to 29.1503° N (Figure 2). Larvae were collected using multiple sampling gears. A Tucker trawl (1 x 1.4 m) was towed at three discrete depths (1, 10, and 20 m), and a rectangular net (1 x 2 m) was towed horizontally through the water column. Additionally, a ring net (0.6 m diameter) was towed at the surface, and a bongo net (60 cm OD) was towed obliquely from 0-30 m depth. All nets were fitted with 333 µm mesh netting. Net tow duration was approximately 10 min at a target vessel speed of two knots.

The second study area was larger but contained within the US EEZ and bounded by longitudes 81.4645° to 96° W and latitudes 24.3917° to 29.5° N. Sampling was carried out during

24-hour operations from 30 April through 29 May 2012 beyond the 200 m depth contour. The survey was part of the SEAMAP spring plankton survey with some additional stations sampled (Millet 2012) (SEAMAP dataset henceforth). Two rectangular nets (1 x 2 m) were used, one outfitted with 947 µm mesh netting that targeted the neuston layer and a second net outfitted with 505 µm mesh netting that undulated between 0-10 m for 10 min intervals (Habtes et al. 2014). The latter net was fitted with a mechanical flowmeter (2030R, General Oceanics, Inc) attached at the center of the net to record volume filtered. For additional sampling methodology in the GOM, see Laiz-Carrión et al. (2015). All samples (GCRL and SEAMAP datasets) were fixed in 95% ethanol and transferred to 95% or 70% ethanol respectively.

Larval BFT were identified using morphological characteristics retained after ethanol preservation (Richards et al. 1990, Richards 2005, Puncher et al. 2015) and verified by a senior taxonomist. Body length (BL) was measured as standard length (SL) or notochord length (NL) following Brothers et al. (1983) to the nearest 0.05 mm. Shrinkage is known to occur when preserving fish larvae in ethanol, but it was assumed constant and proportional for all fish in this study.

2.2. Otolith preparation and interpretation

A subset of all larvae collected in the GOM were selected to represent the spatial distribution within the US EEZ (Figure 2). Otoliths were extracted from larval BFT using minuten needles or sharpened glass probes, then cleaned, dried and transferred into one drop of mounting medium (Flo-Texx^{TM}), with the distal side facing up. Sagittal otoliths were chosen for ageing because they are the largest (and easiest to extract) amongst the three types of otoliths observed (Itoh et al. 2000). Similar to observations by García et al. (2006), the sagittae and lapilli resembled each other in shape and size; therefore, the otolith with the larger otolith radius (OR) was

determined to be the sagittal otolith (Figure 3). Previous ageing studies conducted for a variety of fishes found no significant differences between age estimates derived from the left versus the right otolith (Campana 1999), thus one sagittal otolith from each larva was randomly selected for ageing. The OR was measured from the center of the primordium to the longest axis. Sub-daily increments were avoided by only counting D-zones which were continuous for at least 50% of the individual increment's circumference.

Sagittal otoliths were examined with a compound microscope at 400-1000x with immersion oil under transmitted light, and daily increments were counted twice along the OR. For the GCRL otoliths, two readers independently examined each otolith. If the readers did not reach a consensus, those counts were removed. For the SEAMAP dataset, increments were read by three independent readers using digitized images captured by an Olympus BH2 compound microscope at 1000x and image analysis software (Image Pro Plus 7). Mean value of increment reads was calculated and rounded down to nearest 0.5.

Suitable age estimations of larval tunas (*Thunnus*) must consider that the first daily increment observed is not equivalent to day-1 of life. This offset is because the primordium is surrounded by an optically "diffuse zone" that comprises discontinuous but non-incremental growth (Brothers et al. 1983, Itoh et al. 2000) until the first daily increment develops. A timeline of larval BFT growth was developed to obtain an age correction to the increment counts by consulting larval *Thunnus* studies. Tanaka et al. (2014a; 2014b) indicated that *T. orientalis* eggs hatch within 48 hours, with mouth development and exogenous feeding taking place between 3 and 4 days post hatch (dph). The onset of exogenous feeding in *T. orientalis* was also concurrent with formation of the first daily increment (Kawamura et al. 2003). Previous age estimates for larval BFT concluded that 3 to 4 days was suitable correction (Brothers et al. 1983, Itoh et al.

2000) to calculate dph; however, a recent hatchery study indicated that warmer temperatures reduced hatching time by half for BFT eggs exposed to 26 °C vs 19.5 °C (Gordoa et al. 2014).

Additionally, Yúfera et al. (2014) observed that exogenous feeding began 2 dph for larval BFT reared at 23–24 ºC. Therefore, in the warm waters (mean SST > 25 ºC) of the GOM during the sampled spawning seasons, hatching and development is likely accelerated. For this study, 2 days were added to the final increment count in order to estimate dph. Measurements of precision between readers for the SEAMAP dataset were calculated using the Chang's (1982) coefficient of variation (CV), adjusted by adding 2 days.

Least squares regressions were calculated for best fit of BL to number of daily increments and for best fit of BL to OR following Brothers et al. (1983). In addition, datasets from previous BFT ageing studies conducted using larvae collected from the SOF (Brothers et al. 1983) and the Balearic Sea (García et al. 2013) were analyzed as generously provided by those authors (Table 1). The BL for larvae collected from the Balearic Sea was measured from freshly defrosted specimens and adjusted for ethanol-induced shrinkage by the following formula adapted from Satoh et al. (2008) for *T. orientalis*:

$$BL_{ethanol} = \frac{(BL_{frozen} - 0.67)}{0.96}$$

Length at age relationships were tested using a 2-way analysis of covariance (ANCOVA) run using R 3.2.3 (R Core Team, 2015) with increment counts utilized as a continuous covariate. To compare overall growth, the slopes of each curve were tested first within the GOM datasets (GCRL and SEAMAP) and then between the GOM, SOF, and Balearic Sea datasets. Otolith size between the GOM, SOF and Balearic Sea datasets was also analyzed using an ANCOVA for the log-transformed values of OR with BL as a covariate.

2.3. Otolith microstructure analysis

Otoliths were measured from the approximate center of the primordium to the edge of the diffuse zone (non-incremental region) as described by Itoh et al. (2000) and successively to the edge of each D-zone along the OR at 1000x (Figure 3). Increment widths (IW, μm) were measured in both the GCRL and the SEAMAP datasets using image analysis software (ImageJ, National Institute of Health, Bethesda, MD and the Otolith Macro^{TM}, Media Cybernetics, Inc., respectively). An increment was determined as complete when the beginning of the subsequent L-zone was apparent. Otoliths with CV values larger than 15% were not included in the microstructure analyses.

The IW for the Balearic Sea dataset from 2003, 2004 and 2005 were measured using the OTO program (Andersen & Moksness 1988, for more detail see García et al. 2013). Differences for IW among the three datasets were tested using permutational multivariate analysis of variance (PERMANOVA) in PRIMER 6 software (Anderson, 2001; Anderson & Robinson 2003; Clarke & Gorley 2001; 2006), first between the two GOM datasets (GCRL and SEAMAP), then among the Balearic Sea 2003, 2004 and 2005 datasets, and lastly between GOM and Balearic Sea datasets combined. Multivariate analyses used Euclidean distance matrices, and significance was tested using permutation. Measurements of IW were included in the analysis if that increment bin had at least four observations for each increment measured. Within the GOM, increment bins 0 through 9 were examined, while for the GOM and Balaeric Sea analysis, increment bins 1-11 were examined.

3. Results

3.1. Larval collections

BFT larval catches were patchy and variable for both GOM sampling efforts. The GCRL dataset had positive catches ($n \geq 1$) at 21% of stations, and larvae were collected entirely from the eastern GOM (Figure 2). The majority of larvae (80%) measured less than 5 mm SL. The SEAMAP collections had positive catches ($n \geq 1$) at 63% of the 128 stations sampled, and included the eastern and western GOM (Figure 2). Larval sizes for both GOM datasets included pre-flexion larvae; however, the majority (87%) were in flexion and post-flexion developmental stages. Mean BL (SL, mm ± SE) for all aged larvae was 4.76 ± 0.08 and ranged from 2.1 to 10.8 mm.

3.2. Larval ageing

A total of 259 larvae were aged from the two GOM datasets (Table 1). Figure 3 shows images of typical otoliths encountered from the SEAMAP dataset: small (3a), medium (3b) and large (3c). The least squares regression in the linear form was fitted to the daily increment and length data from both GOM datasets ($y = mx + b$, $m = 0.46$, $b = 2.24$, $r^2 = 0.85$, n=259). The observed slope of the line (m) corresponds to the larval BFT population growth rate. Increments ranged from 0 to 15 corresponding to 2 to17 dph (Figure 4). The three oldest larvae (with 13, 14 and 15 increments, respectively) were not included in the calculation of the linear regression but are shown in Figure 4. The mean age was 7.43 days ± 0.17, and the majority (90%) of aged larvae ranged between 2-10 days old. Back-calculated spawning dates began on 16 April and continued almost daily through 22 May. The oldest individuals (10 +days) were all estimated to spawn in the first two weeks of May. The CV for the majority of the SEAMAP dataset (80%) was lower than 10% with an average of 7.41 ± 0.23 (mean ± SE).

No significant difference was found (ANCOVA F [1, 257] = 0.167, p = 0.683) for the slopes of the growth curves between the two GOM datasets. Given the overlap in geographic coverage, depth, sampling strategies and ageing methodologies, the GCRL and SEAMAP datasets were combined in the subsequent analyses (Table 2).

ANCOVA analysis among BFT datasets (GOM, SOF, and Balearic Sea) indicated differences (F (1, 977) = 9.857, p = 0.002) in the slopes of the growth curves and pairwise comparisons showed that larval growth in the GOM was significantly faster than larvae from both the SOF (F [1, 589] = 17.048, p < 0.001), and Balearic Sea (F [1, 645] = 28.200, p < 0.001), Figure 5.

3.3.Otolith microstructure

Otolith biometrics in this study incorporated both smaller and larger larvae OR values when compared to the SOF dataset (Brothers et al. 1983) resulting in a wider range of otolith sizes (Figures 5 and 6). Larval BFT otoliths had a diffuse zone that averaged 9.63 μm ± SE while the OR averaged 27.61 μm ± 1.01 and ranged from 9.73 to 144.80 μm. ROG values ranged from 0.6 - 15.15 μm (4.4 μm ± 0.25). Overall, body length had a positive exponential relationship with OR (Figure 6). The least squares regression in the exponential form was fitted to the observed OR measurements ($y = ae^{bx}$, n =262, a = 5.22, b = 0.32, r^2 = 0.93). The otoliths (log-OR) from GOM specimens were significantly larger than the SOF larvae (F [1, 348] = 22.854, p < 0.001) and the Balearic Sea at similar sizes (F [1, 646] = 8.666, p = 0.003).

Daily larval growth for GOM datasets followed a similar trend (Figure 7) with individuals growing faster as they became older. Daily growth as shown by IW increased quickly up to 6.6 μm BL by increment 9 (Figure 7). Results of pairwise PERMANOVA between the two GOM

datasets indicated that the IW differed significantly ($p = 0.001$) at increments 0–3, but was not significant at increments 4–9 (Table 3a).

IW measurements indicated large and significant differences in daily growth patterns between GOM and Balearic Sea otoliths (PERMANOVA, F [1, 10] = 76.679, $p < 0.001$). GOM otoliths had significantly wider increments beginning at increment 3, continuing through increment 11 ($p < 0.001$) (Table 3b, Figure 7).

Further PERMANOVA analysis comparing IW between the three years of sampling in the Balearic Sea dataset (2003, 2004 and 2005 cohorts) indicated that otolith IW were significantly different among year of collection ($F = 283.71$, $p = 0.001$), and among increment counts ($p = 0.001$). The IW were higher for larvae collected during 2003 (Figure 7) than larvae from 2004 or 2005. Daily growth of larvae between 2004 and 2005 was very similar across the age spectrum examined.

4. Discussion

This study contributes to ongoing efforts to improve our understanding of the larval ecology of BFT with the aim of improving biological parameters utilized in stock assessment models. In particular, this study produced an updated growth curve by ageing larval BFT collected from the GOM, which is the main BFT spawning ground in the western Atlantic. Larval growth was faster than previously described (Brothers et al. 1983) as indicated by age at length measurements obtained from sagittal otoliths. Furthermore, comparisons between published BFT larval growth studies conducted in the SOF (Brothers et al. 1983) and Balearic Sea (García et al. 2013) showed significant differences between growth curves.

Individual growth rates for GOM larvae were variable, with a mean of 0.67 mm d^{-1}, which was higher than reported for BFT larvae collected from the SOF (Brothers et al. 1983) and Balearic Sea (García et al. 2013) when correcting for dph (increment counts + 2). The smaller otolith sizes for SOF larvae when compared to GOM otoliths point to slower growth, and possibly less favorable environmental conditions for BFT larvae growing in the SOF region. The SOF larvae were sourced from a very small geographic area at the inshore edge of the Gulf Stream (Figure 2) near Miami, FL, hundreds of kilometers from the GOM spawning grounds. As a result, the SOF larvae are not representative of the full range of environmental variation that occurs in the GOM during the spring spawning season. In addition, the growth curve derived from Brothers et al. (1983) lacks appropriate smaller size classes (<4 mm). This is possibly due to the use of a coarser mesh size (950 µm) than that used for GOM collections (333 and 505 µm), as well as the distance of the Florida collection locations from the main GOM spawning ground. Finally, the smaller OR for Balearic Sea otoliths also supports slower larval growth when compared to the GOM during early growth. These morphometric comparisons are the first incidence of comparing the two main spawning grounds using larval otolith metrics and should be examined further particularly for larger larval BFT.

The growth curve described in this study is a substantial improvement over the Brothers et al. (1983) growth curve because: 1) it includes larvae from across the spatial range of the main GOM spawning ground and the temporal range during the spawning activity although aged larvae from the east GOM are more numerous, and 2) it includes a wider range of size classes and consequently better reflects variability in larval ages. This improved growth curve can be implemented in models for example in the formulation of the larval BFT index, which is currently the only fishery-independent data input to the western BFT stock assessment (Ingram et al., 2010).

Larval growth rates from the GOM were also significantly faster than in the Balearic Sea studies. This was particularly evident for otolith IW. Larvae from the two regions showed similar growth trajectories at younger ages, but there was large and significant separation between the daily growth trajectories at larger sizes (> 6 mm), indicating marked differences in larval growth. Mean IW from GOM larvae at larger sizes were more than twice those from similarly aged larvae from the Balearic Islands. These differences in early growth patterns between the two spawning grounds may have important ecological implications for recruitment dynamics and could result in the presence of different larval survival mechanisms between the two ecosystems (Laiz-Carrión et al. 2015, Tilley et al. 2016). Faster BFT larval growth for GOM individuals could provide an opportunity for enhanced survival during the most vulnerable stages, as long as sufficient food is available.

The onset of exogenous feeding is a crucial moment in larval survival and marks the beginning of larval growth (Yúfera and Darias 2007). Scombrids have high but variable larval growth rates that are influenced by the surrounding environment (Tanaka et al. 2006). Timing of first increment formation has been linked with first exogenous feeding for Pacific BFT (Itoh et al. 2000, Kawamura et al. 2003, Gordoa & Carreras 2014). Average larval growth rates for the GOM (0.46 mm inc^{-1}) were higher than *T. orientalis* from the Northwest Pacific Ocean (0.3-0.5 mm d^{-1}, Tanaka et al. 2006) and *T. maccoyii* from the Indian Ocean (0.32 mm d^{-1}, Jenkins & Davis 1990). By way of comparison, Yellowfin Tuna (*T. albacares*) from the GOM (Lang et al. 1994) had similar growth rates to BFT (0.47 mm d^{-1}), as did *Katsuwonus pelamis* (0.51 mm d^{-1}, Zygas et al. 2015). This suggests that environmental conditions in the GOM may support particularly fast growth for tuna larvae.

Despite some environmental similarities between the GOM and Balearic Sea, spawning grounds (Muhling et al. 2013), BFT larvae from each of these two regions displayed differences in growth that may reflect differing ecological processes. One of the main differences between the spawning grounds is the warmer temperatures in the GOM. García et al. (2013) showed that warm anomalies in the western Mediterranean during the 2003 spawning season resulted in higher growth rates when compared to subsequent years (2004 and 2005) for that cohort. The 2003 cohort has resulted in the strongest year class in recent years (Suzuki et al. 2013). Atlantic BFT larvae raised in laboratory experiments at higher temperatures also had larger otoliths and displayed greater somatic growth rates than those raised at lower temperatures (Mendiola & Álvarez 2008). Additional laboratory and field experiments to isolate the effects of ambient water temperature on growth of larval BFT in combination with other factors (e.g. prey fields, maternal condition) may be required to assess this further.

Differences in prey type and availability may also be important in the observed differences between the GOM and Balaeric growth patterns. For instance, Laiz-Carrión et al. (2015) found differences in the isotopic values of tissues from BFT larvae from the GOM and the Balearic Sea, which suggested different nitrogen sources and food web structure in the two regions. In addition, a major contributor to the observed differences in growth may be the early onset of piscivory for GOM BFT starting at approximately 6 mm BL (Llopiz et al. 2014). Piscivory has also been observed in Pacific BFT, starting at ~8mm BL (Tanaka et al. 2014b), but has not been documented in wild BFT larvae from the Mediterranean Sea (Catalan et al. 2011, Laiz-Carrión, pers com). The initiation of piscivory (~7-8+ days) coincides with the onset of the divergence of growth histories observed between GOM and Balearic Sea larvae. Laiz-Carrión et al. (2015) reported that the Mediterranean Sea larvae were heavier (mass) than the GOM BFT larvae at a similar size (BL)

which may indicate slower growth rates in the Mediterranean larvae, yet faster growth in the GOM. Our study also analyzed larvae from 2012 which is the same spawning year analyzed by Laiz-Carrión et al. (2015) but also included larvae from 2000-2010 (GCRL dataset), and our study found faster growth in the GOM supporting their study's conclusions but augmenting it using otolith growth comparisons.

These differences between larval BFT from each spawning ground suggest that larvae from each ecosystem exhibit different strategies during early life history with two very well differentiated growth strategies, with Balearic Sea larvae acquiring more body mass with time while the GOM larvae are more slender and faster growing. The two stocks may also have differing susceptibility to environmental variability on spawning grounds that may result in uneven contributions of eastern vs western BFT stock to the adult population each year (Secor et. al 2013). For example, while sea surface temperatures between the two ecosystems were on average similar, concurrent shipboard measurements from the GOM had higher variability (± 3.3°C) when compared to any of the Balearic Sea datasets (2003-2005) and as a result, GOM BFT larvae experienced wider and warmer range of temperatures. For example, the aged GOM larvae included 123 otoliths collected in surface temperatures above 27°C, while that range of surface temperatures was only experienced by a mere 20 larvae from the combined 2003, 2004 and 2005 cohorts in the Balearic Sea.

Adult BFT are capable of transatlantic movements and likely target specific spawning locations, including favorable habitats with suitable prey resources for their larvae. Warm waters with low chlorophyll levels characterize BFT spawning grounds, as spawning takes place following the seasonal warming period when temperatures reach approximately 24°C (Muhling et al. 2010). Little is understood about the effect of these environmental drivers on daily growth of

larvae developing in the GOM. Back-calculated spawning dates from the SEAMAP dataset indicate that weekly and likely daily spawning events took place in the GOM during the 2012 spawning season. Examination of field collected larval Pacific BFT showed that an increase in water temperature was associated with increased larval growth, but only provisionally and only detected later in larval life (Tanaka et al. 2006). Pepin (1990) also found that temperature facilitates larval development but observed that temperature variations did not appear to have a net effect on larval survival. Overall, it is challenging to disentangle the influence of environmental variables on larval BFT growth in the GOM given the large extent of the region. Future ageing studies may benefit by not only relating concurrent environmental variables, but also including naturally occurring gradients to characterize already observed relationships between larval growth and the oceanographic environment in other congener larval tunas.

Several knowledge gaps and needs for further research were identified by this study. The SEAMAP surveys target the BFT spawning season (April-May), but spawning likely continues into June. Future larval ageing efforts should determine BFT larval growth rates during June. In addition, a review of timing of first daily increment formation for GOM BFT is necessary given the application of using larval age in stock assessment and back-tracking models. Larval BFT growth should also be examined within the spatial structure of mesoscale and sub-mesoscale oceanographic features typically found in the GOM ecosystem. These features accumulate both prey and predators (Lindo-Atichati et al. 2012) and influence larval growth rates for larvae of other fish species (Shulzitski et al. 2012). Furthermore, additional sampling to define the influence of interannual variability on larval BFT growth rates in GOM is required, as our results included only one cruise with high spatial coverage (2012). While the 2012 spawning season was not an unusual year in the GOM in terms of oceanography or environmental conditions (Muller-Karger et al.

2015), quantification of interannual variability among BFT cohorts would improve the robustness of our results.

The current study substantially improved current understanding of larval BFT growth and ecology in the GOM. We updated the existing larval BFT growth curve by using age data from a broader size range of larvae collected from the GOM spawning grounds throughout the BFT spawning season. Our findings will improve the larval index of spawning biomass to be incorporated in future BFT stock assessments. Our results also identified strong differences in larval growth rates between the GOM and Balearic Islands spawning grounds, which may be linked to larval feeding ecology. Baseline growth rates for BFT larvae in the GOM can be utilized to compare and evaluate larval growth from collections outside of the main spawning grounds. These advances will contribute significantly to improving knowledge of larval ecology and recruitment processes for BFT in the Atlantic, and to the sustainable management of this species.

Acknowledgments

We wish to thank the captains and crews of all vessels that collected plankton samples in the Gulf of Mexico, particularly the NOAA Ship Gordon Gunter and the University of Southern Mississippi's R/V Tommy Munro. In addition, we extend our gratitude to the field-going and land-based staff at the NOAA-NMFS Pascagoula Laboratory, the Gulf Coast Research Lab (in particular D. Gibson), and particularly the NOAA-Miami Laboratory, FORCES Unit. This work was supported by the National Aeronautics Space Administration (NX11AP76G S07), the National Oceanic and Atmospheric Administration – Bluefin Tuna Research Program (NA15NMF4720110), "ECOLATUN" MINECO/FEDER (#CTM2015-68473-R), and by the Guy Harvey Ocean Foundation (to J. Franks). The funders had no role in study design, data collection and analysis, decision to publish, or preparation of the manuscript. Helpful comments were provided by J.M. Quintanilla, R. Laiz-Carrión, L. Rasmuson, and K. Shulzitski.

References

Alemany, F., Quintanilla, L., Velez-Belchí, P., García, A., Cortés, D., Rodríguez, J.M., Fernández de Puelles, M.L., González-Pola, C., López-Jurado, J.L., 2010. Characterization of the spawning habitat of Atlantic bluefin tuna and related species Balearic Sea (western Mediterranean). Prog. Oceanogr. 86:21–38.

Andersen, T., Moksness, E., 1988. Manual for reading daily increments by the use of a computer program. Flødevigen Meldingen. 4:1–37.

Anderson, M.J., 2001. A new method for non-parametric multivariate analysis of variance. Austral. Ecol. 26: 32-46.

Anderson, M.J., Robinson, J., 2003. Generalized discriminant analysis based on distances. Aust. N. Z. J. Stat. 45: 301-318.

Anonymous, 2014. Report of the 2014 Atlantic Bluefin Tuna Stock Assessment Session. Report ICCAT. 1–178.

Block, B.A., Teo, S.L.H., Walli, A., Boustany, A., Stokesbury, M.J.W., Farwell, C.J., Weng, K.C., Dewar, H, Williams, TD., 2005. Electronic tagging and population structure of Atlantic bluefin tuna. Nature. 434:1121-1127.

Brothers, E.B., McFarland, W.N., 1981. Correlations between otolith microstructure, growth, and life history transitions in newly recruited French grunts [*Haemulon flavolineatum* (Desmarest), Haemulidae]. Rapp. p-v Reun. Cons. Int. Explor. Mer. 178:369-374.

Brothers, E.B., Prince, E.D., Lee, D.W., 1983. Age and growth of young-of-the-year blue fin tuna, *Thunnus thynnus*, from otolith microstructure. In: Prince ED and Pulos LM eds) Procedures of the international workshop on age determination of oceanic pelagic fishes: tunas, billfishes, and sharks. NOAA Tech. Repos. N M F S. 8:49-60.

Butler, C.M., Logan, J.M., Provaznik, J.M., Hoffmayer, E.R., Staudinger, M.D., Quattro, J.M., Roberts, M.A., Ingram, G.W. Jr, Pollack, A.G., Lutcavage, M.E., 2015. Atlantic bluefin tuna *Thunnus thynnus* feeding ecology in the northern Gulf of Mexico: a preliminary description of diet from the western Atlantic spawning grounds. J. Fish. Bio. 86:365–374 doi:10.1111/jfb.12556.

Campana, S.E., Jones, C., 1992. Analysis of otolith microstructure data. In: Stevenson DK, Campana SE (eds) Otolith microstructure examination and analysis. Can. Spec. Publ. Fish. Aqu. Sci. 117:73-100.

Campana, S.E., 1999. Chemistry and composition of fish otoliths: pathways, mechanisms and applications. Mar. Ecol. Prog. Ser. 188:263-297.

Catalan, I., Tejedor, A., Alemany, F., Reglero, P., 2011. Trophic ecology of Atlantic bluefin tuna *Thunnus thynnus* larvae. J. Fish Biol. 78:1545–1560.

Chang, W.Y.B., 1982. A statistical method for evaluating the reproducibility of age determination. Can. J. Fish. Aquat. Sci. 39:1208-1210.

Clarke, K.R., Gorley, R.N., 2001 & 2006. PRIMER v6: user manual/tutorial. PRIMER-E, Plymouth.

Fiksen, Ø., Jørgensen, C., Kristiansen, T., Vikebø, F., Huse, G., 2007. Linking behavioural ecology and oceanography: larval behaviour determines growth, mortality and dispersal. Mar. Ecol. Prog. Ser. 347:195-205.

Fromentin, J.M., Powers, J.E., 2005. Atlantic bluefin tuna: population dynamics, ecology, fisheries and management. Fish Fish 6:281-306.

García, A., Cortes, D., Ramírez, T., Fehri-Bedoui, R., Alemany, F., Rodríguez, J.M., Carpena, A., Alvarez, J.P., 2006. First data on growth and nucleic acid and protein content of field-captured Mediterranean bluefin (*T. thynnus*) and albacore (*T. alalunga*) larvae: a comparative study. Sci. Mar. 70S2:67-78.

García, A., Cortés, D., Quintanilla, J., Rámirez, T., Quintanilla, L., Rodríguez, J.M., Alemany, F., 2013. Climate-induced environmental conditions influencing interannual variability of Mediterranean bluefin (*Thunnus thynnus*) larval growth. Fish. Oceanogr. 22(4):273-287.

Gordoa, A., Carreras, G., 2014. Determination of temporal spawning patterns and hatching time in response to temperature of Atlantic bluefin tuna (*Thunnus thynnus*) in the Western Mediterranean. PLoS ONE 9(3):1-9.

Habtes, S., Muller-Karger, F., Roffer, M., Lamkin, J.T., Muhling, B.A., 2014. A comparison of sampling methods for larvae of medium and large epipelagic fish species during spring SEAMAP ichthyoplankton surveys in the Gulf of Mexico. Limnol. Oceanog. Meth. 12:86-101.

Hare, J.A., Cowen, R.K., 1997. Size, growth, development, and survival of the planktonic larvae of *Pomatomus saltatrix* (Pisces: Pomatomidae). Ecology 78(8): 2415-2431.

Ingram, G.W., Richards, W.J., Lamkin, J.T., Muhling, B.A., 2010. Annual indices of Atlantic bluefin tuna (*Thunnus thynnus*) larvae in the GOM developed using delta-lognormal and multivariate models. Aqua. Living. Res. 23:35-47.

Itoh, T., Shiina, Y., Tsuji, S., Endo, F., Tezuka, N., 2000. Otolith daily increment formation in laboratory reared larval and juvenile bluefin tuna *Thunnus thynnus*. Fish. Sci. 66(5):834-839.

Jenkins, G.P., Davis, T.L.O., 1990. Age, growth rate, and growth trajectory determined from otolith microstructure of southern bluefin tuna *Thunnus maccoyii* larvae. Mar. Ecol. Prog. Ser. 63, 93–104.

Kawamura G., Masuma S., Tezuka N., Koiso M., Jinbo T., Namba K., 2003. Morphogenesis of sense organs in the bluefin tuna *Thunnus orientalis*. In: Browman HI, Skiftesvik AB (eds) The Big Fish Bang, Inst, Mar, Res,, Bergen, Norway, 123–135.

Laiz-Carrión, R., Gerard, T., Uriarte, A., Malca, E., Quintanilla, J.M., Muhling, B.A., Alemany, F., Privoznik, S., Shiroza, A., Lamkin, J.T., García, A., 2015. Trophic ecology of Atlantic bluefin tuna (*Thunnus thynnus*) larvae from the Gulf of Mexico and NW Mediterranean spawning grounds: a comparative stable isotope study. PLoS ONE. DOI:10.1371/journal.pone.0133406.

Lamkin, J.T., Muhling, B.A., Malca, E., Laiz-Carrión, R., Gerard, T., Privoznik, S., Liu, Y., Lee, S., Ingram, G.W., Roffer, M.A., Muller-Karger, F., Olascoaga, J., Fiorentino, L., Nero, W., Richards, W.J., 2014. Do western Atlantic bluefin tuna spawn outside of the Gulf of Mexico? Results from a larval survey in the Atlantic Ocean in 2013. Col. Vol. Sci. Pap. ICCAT. 176/2014.

Lang, K.L., Grimes, C.B., Shaw, R.F., 1994. Variations in the age and growth of yellowfin tuna larvae, *Thunnus albacares*, collected about the Mississippi River plume. Environ. Biol. Fish., 39: 259–270.

Lindo-Atichati, D., Bringas, F., Goni, G., Muhling, B., Muller-Karger, F.E., Habtes, S., 2012. Varying mesoscale structures influence larval fish distribution in the northern Gulf of Mexico. Mar. Ecol. Prog. Ser. 463:245-257.

Llopiz, J.K., Muhling, B.A., Lamkin, J.T., 2014. Feeding dynamics of Atlantic Bluefin tuna (*Thunnus thynnus*) larvae in the Gulf of Mexico. Col. Vol. Sci. Pap. ICCAT. 173/2014.

Lyczkowski-Shutlz, J., Hanisko, D.S., Sulak, K.J., Konieczna, M., Bond, P.J., 2013. Characterization of ichthyoplankton in the Northeastern Gulf of Mexico from SEAMAP plankton surveys, 1982-1999. Gulf. Caribb. Res. 25:1-56.

McGowan M.F., Richards W.J.R., 1989. Bluefin Tuna, *Thunnus thynnus*, Larvae in the Gulf Stream off the southeastern United States: satellite and shipboard observations of their environment. Fish. Bull.87:615-631.

Medina, A., Goñi, N., Arrizabalaga, H., Varela, J.L., 2015. Feeding patterns of age-0 bluefin tuna in the western Mediterranean inferred from stomach-content and isotope analyses. Mar. Ecol. Prog. Ser. 527:193-204.

Mendiola, D., Álvarez, P., 2008. Validation of daily increments in the otolith microstructure of Northeast Atlantic mackerel fish larvae. Fish. Res. 89(3):300-304.

Millet. A., 2012. Southeast Area Monitoring and Assessment Program 2012 Spring Plankton Survey. Cruise Rep. GU-12-01(66):1-50.

Muhling, B.A., Lamkin, J.T., Roffer, M.A., 2010. Predicting the occurrence of bluefin tuna (*Thunnus thynnus*) larvae in the northern GOM: Building a classification model from archival data. Fish. Oceanogr. 19:526-539.

Muhling, B.A., Lee, S.-K., Lamkin, J.T., Liu, Y., 2011. Predicting the effects of climate change on bluefin tuna (*Thunnus thynnus*) spawning habitat in the Gulf of Mexico. ICES J. Mar. Sci. 12 p. doi:10.1093/icesjms/fsr008.

Muhling, B.A., Reglero, P., Ciannelli, L., Alvarez-Berastegui, D., Alemany, F., Lamkin, J.T., Roffer, M.A., 2013. Comparison between environmental characteristics of larval bluefin tuna *Thunnus thynnus* habitat in the GOM and western Mediterranean Sea. Mar. Ecol. Prog. Ser. 486:257-276.

Muller-Karger, F.E., Smith, J.P., Werner, S., Chen, R., Roffer, M., Liu, Y., Muhling, B.A., Lindo-Atichati, D., Lamkin, J.T., Cerdeira-Estrada, S., Enfield, D.B., 2015. Natural variability of surface oceanographic conditions in the offshore Gulf of Mexico. Prog. Oceanogr. 134: 54-76.

Pepin, P., 1990. Effect of temperature and size on development, mortality, and survival rates of the pelagic early life history stages of marine fish. Can. J. Fish. Aquat. Sci. 48:503-518.

Puncher, G.N., Alemany, F., Arrizabalaga, H., Cariani, A., Tinti, F., 2015. Misidentification of bluefin tuna larvae: a call for caution and taxonomic reform. Rev. Fish. Biol. Fish. doi:10.1007/s11160-015-9390-1.

Quintanilla, J.M., Laiz-Carrión, R., Uriarte, A., García, A., 2015. Influence of trophic pathways on daily growth patterns of Western Mediterranean anchovy (*Engraulis encrasicolus*) larvae. Mar. Ecol. Prog. Ser. 531.

R Core Team, 2015. R: A language and environment for statistical computing. R Foundation for Statistical Computing, Vienna, Austria. ISBN 3-900051-07-0, http://www.R-project.org/.

Reglero P., Ortega, A., Blanco, E., Fiksen, Ø. Viguri, F.J., de la Gándara, F., Seoka, M., Folkvord, A., 2014. Size-related differences in growth and survival in piscivorous fish larvae fed different prey types. Aquaculture 433: 94-101.

Richards, W.J., 1976. Spawning of bluefin tuna (*Thunnus thynnus*) in the Atlantic Ocean and adjacent seas. Col. Vol. Sci. Pap. ICCAT. 5:267–278.

Richards, W.J., Potthoff, T., Kim, J., 1990. Problems identifying tuna larvae species (Pisces: Scombridae: *Thunnus*) from the Gulf of Mexico. Fish. Bull. US. 88(3):607–609.

Richards, W.J. (Ed). 2005. Early stages of Atlantic fishes. An identification guide for the Western Central North Atlantic. CRC, Taylor and Francis Group L.L.C. 2591 p.

Richardson, D.E., Marancik, K.E., Guyon, J.R., Lutcavage, M.E., Galuardi, B., Lam, C.H., Walsh, H.J., Wildes, S., Yates, D.A., Hare, J.A., 2016. Discovery of a spawning ground reveals diverse migration strategies in Atlantic bluefin tuna (*Thunnus thynnus*). PNAS. 113: 3299-3304.

Restrepo, V.R., Diaz, G.A., Walter, J.F., Neilson, J.D., Campana, S.E., Secor, D., Wingate, R.L., 2010. Updated estimate of the growth curve of Western Atlantic bluefin tuna. Aquat. Livi. Res. 23:335-342.

Rooker, J.R., Alvarado, Bremer, J.R., Block, B.A., Dewar, H., De Metrio, G., Corriero, A., Kraus, R.T., Prince, E.D., Rodríguez Martín, E., Secor, D.H., 2007. Life History and Stock Structure of Atlantic Bluefin Tuna (*Thunnus thynnus*). Rev. Fish. Sci. 15:265–310.

Rooker, J.R., Secor, D.H., De Metrio, G., Schloesser, R., 2008. Natal homing and connectivity in Atlantic bluefin tuna populations. Science. 322(5902):742-744.

Satoh, K., Tanaka, Y., Iwahashi, M., 2008. Variations in the instantaneous mortality rate between larval patches of Pacific bluefin tuna *Thunnus orientalis* in the northwestern Pacific Ocean. Fish. Res. 89:248-256.

Scott, G.P., Turner, S.C., Grimes, C.B., Richards, W.J., Brothers, E.B., 1993. Indices of larval bluefin tuna, *Thunnus thynnus*, abundance in the GOM: Modeling variability in growth, mortality, and gear selectivity: Ichthyoplankton methods for estimating fish biomass. Bull. Mar. Sci. 53:912-929.

Secor, D.H., Dean, J.M., Campana, S.E., 1995. Recent developments in fish otolith research. Univ. of South Carolina Press, Columbia, SC, USA.

Secor, D.H.,Wingate R.L., Neilson J.D., Rooker J.R., Campana S.E., 2008. Growth of Atlantic bluefin tuna: direct age estimates. Col Vol Sci Pap ICCAT 2008/84.

Secor, D.H., Rooker, J.R., Neilson, J.D., Busawon, D., Gahagan, B., Allman, R., 2013. Historical Atlantic Bluefin tuna stock mixing within fisheries off the United States 1976-2012. Col. Vol. Sci. Pap. ICCAT. 69(2):938-946.

Shulzitski, K., Sponaugle, S., Hauff, M., Walter, K., D'Alessandro, E., Cowen, R.K., 2012. Close encounters with eddies: oceanographic features increase growth of larval reef fishes during their journey to the reef. Biol. Letters. 11:20140746.

Sponaugle, S., 2010. Otolith microstructure reveals ecological and oceanographic processes important to fisheries management. Environ. Biol. Fish. 89: 221-238.

Suzuki, Z., Kimoto, A., Sakai, O., 2013. Note on the strong 2003 year-class that appeared in the Atlantic Bluefin fisheries. Col. Vol. Sci. Pap. ICCAT. 69(1):229-234.

Tanaka, Y., Satoh, K., Iwahashi, M., Yamada, H., 2006. Growth-dependent recruitment of Pacific bluefin tuna *Thunnus orientalis* in the northwestern Pacific Ocean. Mar. Ecol. Prog. Ser. 319:225-235.

Tanaka, Y., Minami, H., Ishihi, Y., Kumon, K., Higuchi, K., Eba, T., Nishi, A., Nikaido, H., Shiozawa, S., 2014a. Relationship between prey utilization and growth variation in hatchery-reared Pacific bluefin tuna, *Thunnus orientalis* larvae estimated using nitrogen stable isotope analysis. Aqua. Res. 45:537–545.

Tanaka, Y., Minami, H., Ishihi, Y., Kumon, K., Higuchi, K., Eba, T., Nishi, A., Nikaido, H., Shiozawa, S., 2014b. Differential growth rates related to initiation of piscivory by hatchery-reared larval Pacific bluefin tuna *Thunnus orientalis*. Fish. Sci, Doi: 10.1007/s12562-014-0798-7.

Tilley, J.D., Butler, C.M., Suárez-Morales, E., Franks, J.S., Hoffmayer, E.R., Gibson, D.P., Comyns, B.H., Ingram, G.W., Blake. E.M., 2016. Feeding ecology of larval Atlantic bluefin tuna, *Thunnus thynnus*, from the central Gulf of Mexico. Bull. Mar. Sci. 92(3):000-000.2016.

Wilson, S.G., Jonsen, I.D., Schallert, R.J., Ganong, J.E., Castleton, M.R., Spares, A.D., Boustany, A.M., Stokesbury, M.J.W., Block, B.A., 2015. Tracking the fidelity of Atlantic bluefin tuna released in Canadian waters to the Gulf of Mexico spawning grounds. Can. J. Fish. Aquat. Sci. 72:1–18.

Yúfera, M., Darias, M.J., 2007. The onset of exogenous feeding in marine fish larvae. Aquaculture. 268(1-4):53-63.

Yúfera, M., Ortiz-Delgado, J.B., Hoffman, T., Siguero, I., Urup, B., Sarasquete, C., 2014. Organogenesis of digestive system, visual system and other structures in Atlantic bluefin tuna (*Thunnus thynnus*) larvae reared with copepods in mesocosm system. Aquaculture. 426-427:126–137.

Zenteno, J., Bustos, C., Landaeta, M., 2014. Larval growth, condition and fluctuating asymmetry in the otoliths of a mesopelagic fish in an area influenced by a large Patagonian glacier. Mar. Biol. Res. 10.5:504-514.

Zygas, A.J., Malca, E., Gerard, T., Lamkin, J., 2015. Age-length relationship of larval skipjack tuna (*Katsuwonus pelamis*) in the Gulf of Mexico. Col. Vol. Sci. Pap. ICCAT. 186/2015 p 8.

Figure Captions

Figure 1. Overview of the two larval bluefin tuna (Thunnus thynnus) study areas (colored boxes) in the North Atlantic Ocean: Gulf of Mexico (blue) and western Mediterranean Sea (red).

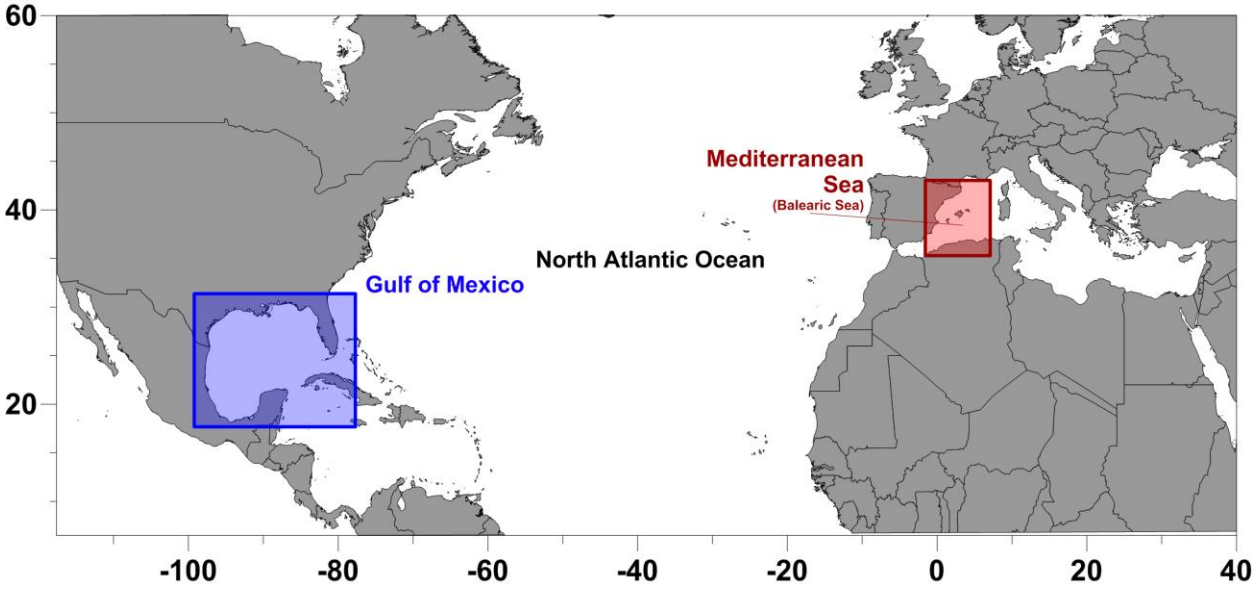

Figure 2: Distribution of sampling locations in the Gulf of Mexico for larval bluefin tuna aged in current study. Symbols specify datasets: all SEAMAP 2012 survey stations (●), SEAMAP stations selected for ageing (+), GCRL stations selected for ageing (**x**). Sampling locations for historic bluefin tuna larvae collected in the Straits of Florida from Brothers et al. (1983) are also shown (▲).

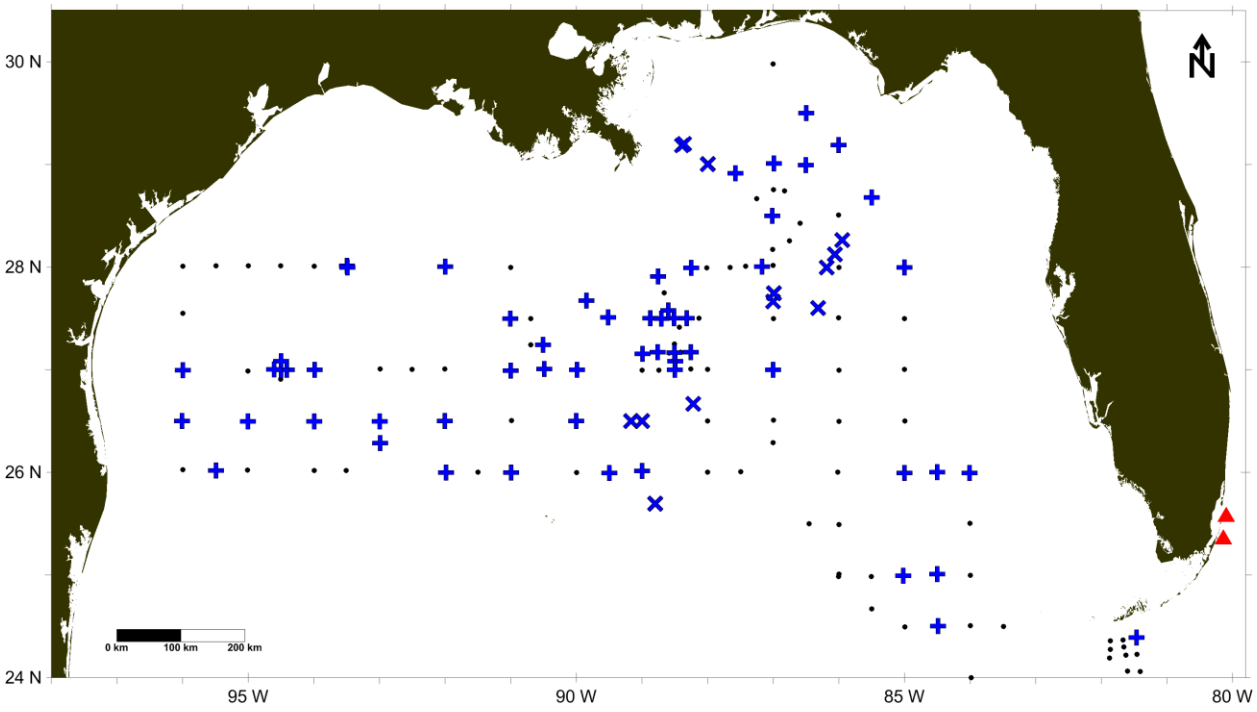

Figure 3: Larval bluefin tuna sagittal otoliths at 1000x under transmitted light: a) 2.6 mm SL larvae with 1 increment b) 5.2 mm SL larvae c) composite image at 1000x of a 8.1 mm SL larva. The primordium (P), otolith radius (OR), diffuse zone (DZ), daily increments (●), increment widths (IW---) and recent otolith growth (ROG) are shown. Scale bars indicate µm.

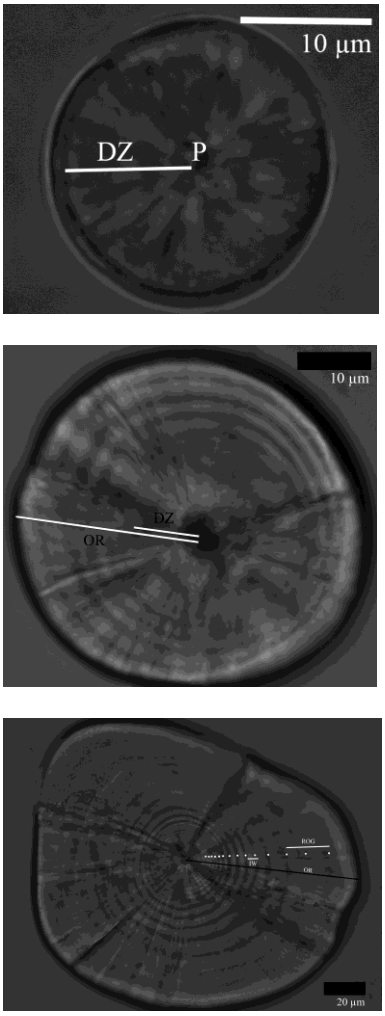

Figure 4. Relationship between otolith daily increments and body length (SL, mm) for bluefin tuna larvae from the Gulf of Mexico. Darker symbol (●) represents individual larvae, gray symbol (●) denotes oldest larvae with n=1 sample sizes. The dotted line is the least squares regression in the linear form and does not include the oldest larvae: y = *mx* + b, n=259, m = 0.463, b = 2.236, r^2 = 0.844.

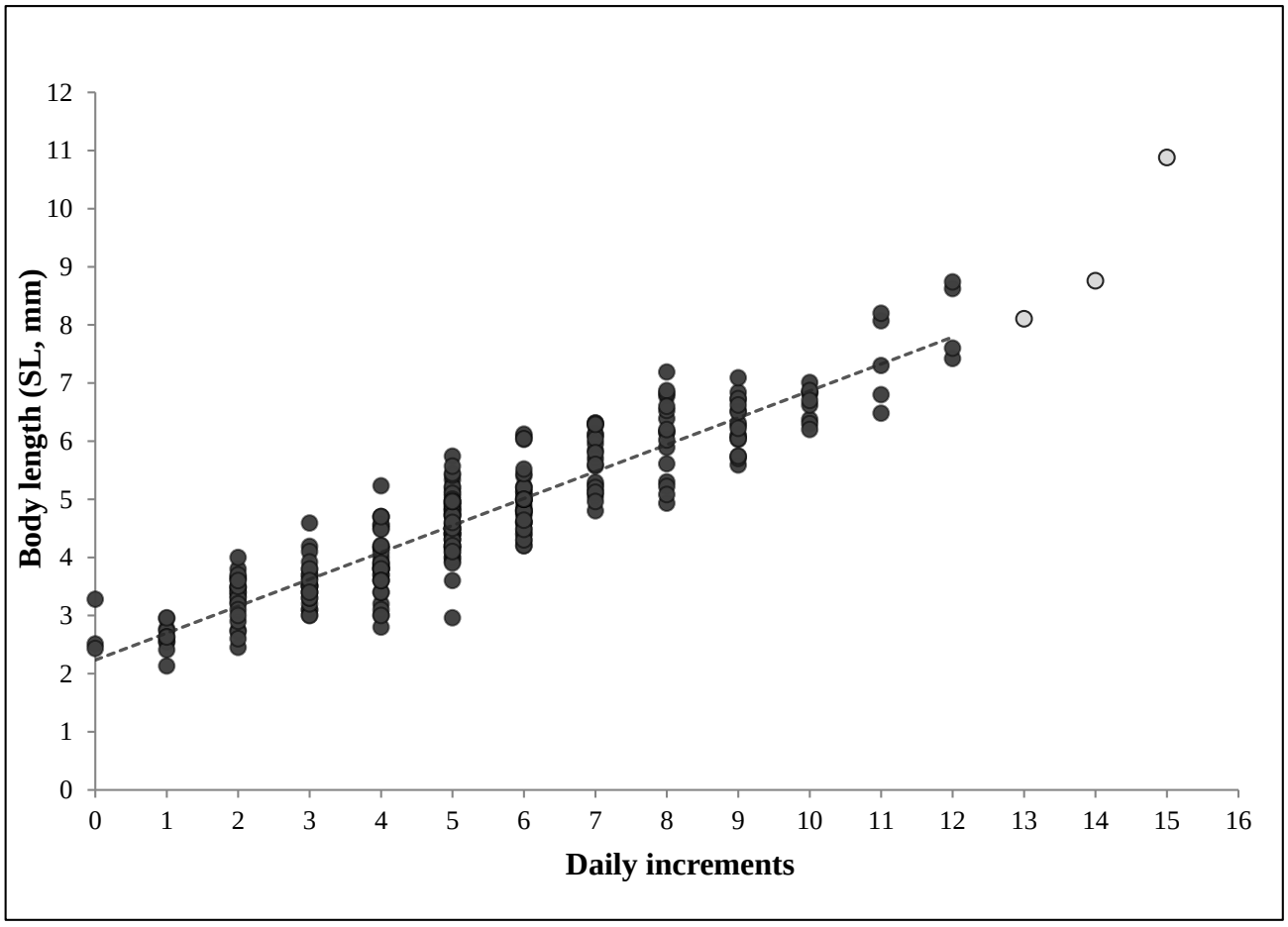

Figure 5. Relationship between otolith daily increments and mean values for body length (SL, mm) for bluefin tuna larvae from the three regions represented: Gulf of Mexico (●), Straits of Florida (▲), and Balearic Sea (■). Dotted lines indicate the least squares regression in the linear form for each dataset, $y = mx + b$.

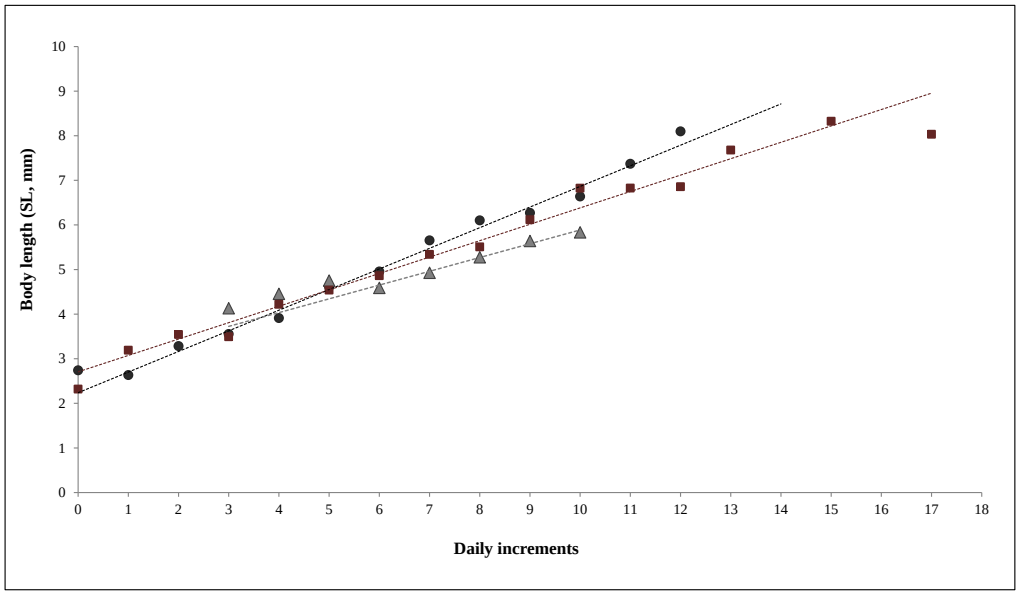

Figure 6. Relationship between body length (NL or SL, mm) of larval bluefin tuna and corresponding otolith radius, µm. Dark circles (●), indicate Gulf of Mexico larvae, triangles (▲) denote larvae from the Straits of Florida (Brothers et al. 1983), square symbols (□) indicate Balearic Sea otoliths. Dotted lines show the least squares regressions in the exponential form $y = ae^{bx}$ for each dataset. Gulf of Mexico regression: N = 262, a = 5.223 b = 0.325 , $r^2 = 0.926$

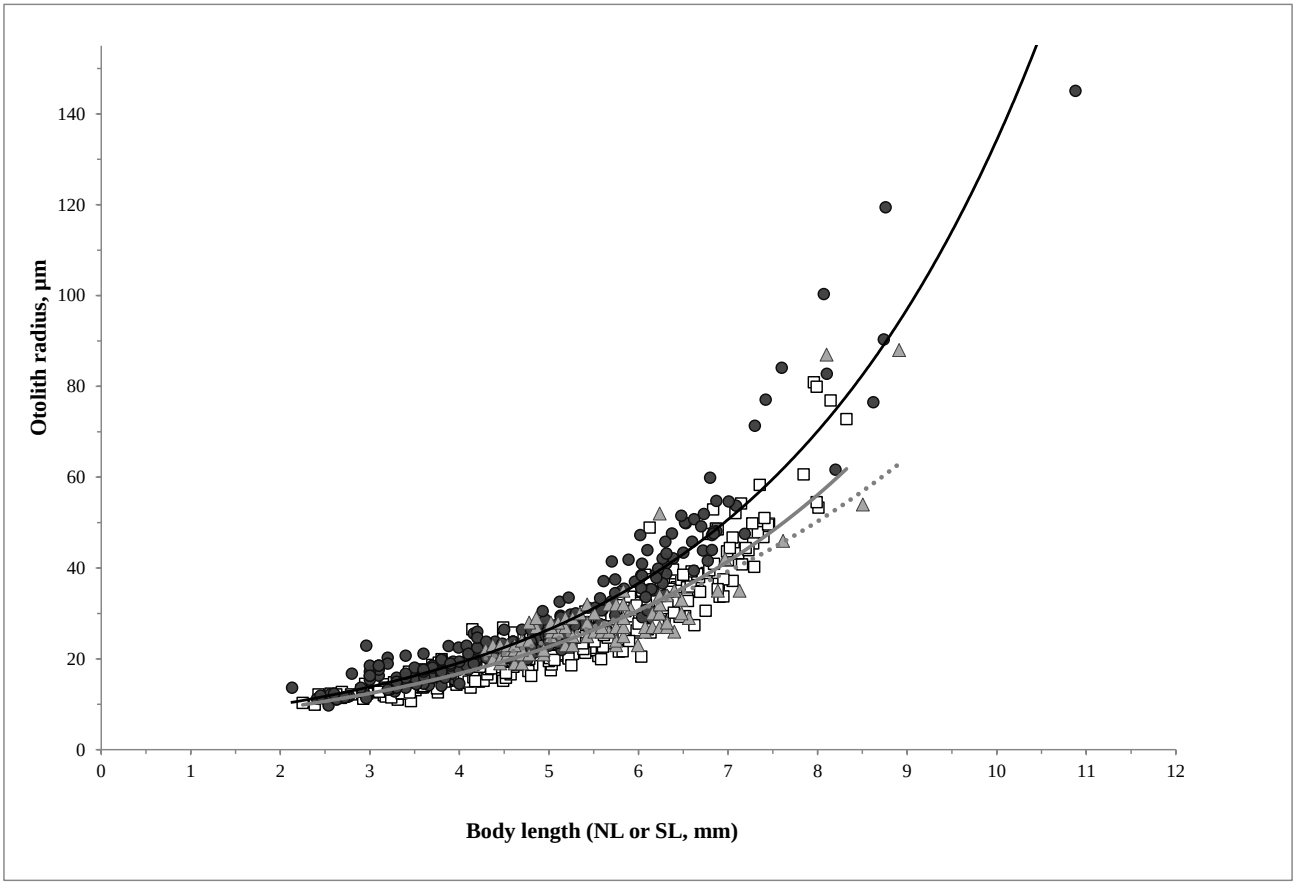

Figure 7. Relationship between daily increments and mean increment width values binned at each individual increment widths (µm) for larval bluefin tuna otoliths n > 2. Two spawning grounds are represented: Gulf of Mexico (●) SEAMAP and GCRL datasets; and Balearic Sea 2003 (■), and combined Balearic Sea 2004-2005 (■) datasets. Error bars indicate standard error.

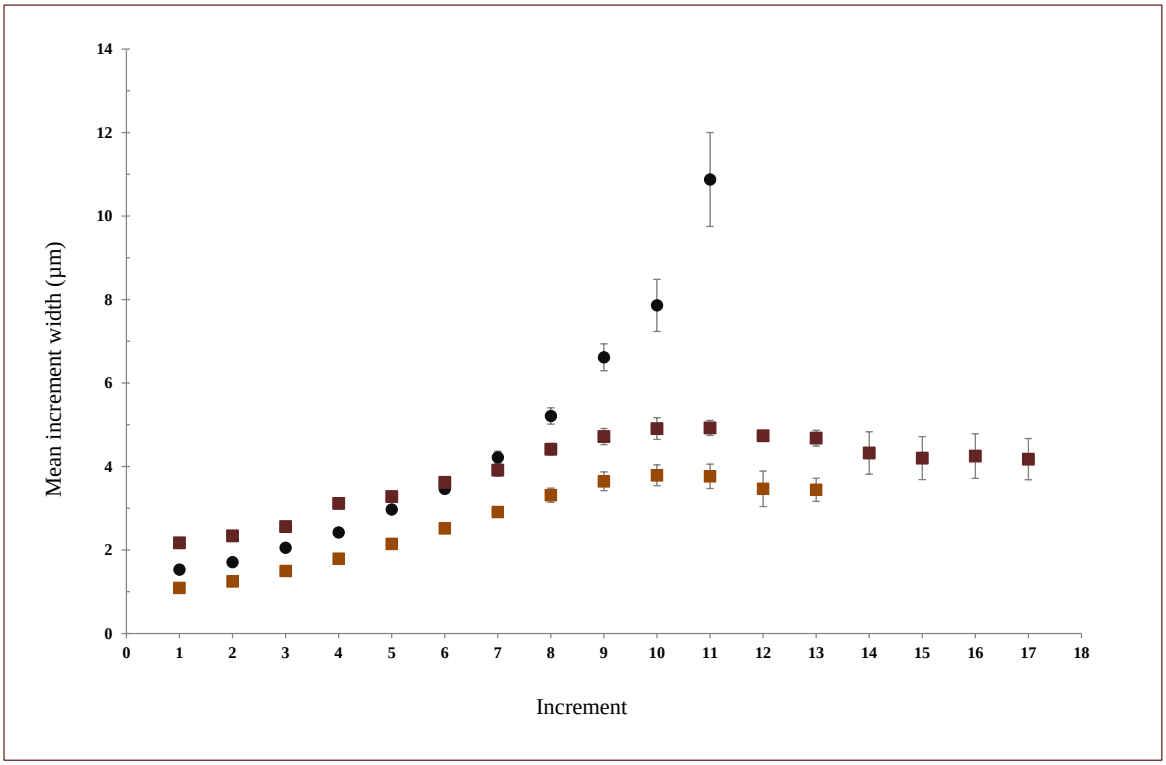

Table 1. Summary of age and growth studies for larval bluefin tuna (*Thunnus thynnus*) in the Northern Atlantic Ocean. Lengths measured for ethanol- preserved larvae. Therefore, the Balearic Sea dataset (García et al. 2013) were adjusted for comparisons (Satoh et al. 2008). Growth rates are the mean ± standard error for SL age^{-1} for each dataset (corrected for dph). Current study is **bolded** for emphasis.

Location	Dataset	Gear (mesh sizes µm)	Aged larvae	Mean growth rate ± SE	Body length, mm		
					mean	min	max
Gulf of Mexico	**GCRL** (128) **SEAMAP** (131)	**Tucker trawl (333), ring net (333), 1 x 2 m rectangular nets (333, 505)**	**259**	**0.67± 0.008**	**4.73**	**2.1**	**10.9**
Straits of Florida	Brothers et al. 1983	1 m rectangular net (505)	334	0.54± 0.003	5.10	3.8	8.9
Balearic Sea (NW Mediterranean)	García et al. 2013	0.9 m bongo (500)	388	0.50 ± 0.004	5.07	2.3	8.3

Table 2. Age at length curve comparisons (ANCOVA) for larval bluefin tuna (*Thunnus thynnus*) in the Atlantic Ocean. Asterisk indicates significant results (p < 0 .001)

Dataset comparisons	*F*	Significance of age at length, p
Gulf of Mexico: SEAMAP vs GCRL	0.167	0.683
Gulf of Mexico (combined) vs Straits of Florida	17.048	4.172e-05*
Gulf of Mexico (combined) vs Balearic Sea	28.200	1.508e-07*
Straits of Florida vs Balearic Sea	1.632	0.202

Table 3. Results for increment width (µm) comparisons for global PERMANOVA and pairwise PERMANOVA a) Gulf of Mexico datasets (GCRL and SEAMAP) for increments 0–9, b) Gulf of Mexico (combined datasets), and Balearic Sea datasets (2003, 2004, and 2005) for increments 1–11. Displayed are pseudo *F*-statistic and p-values based on Euclidean distances from untransformed data. Significant differences ($p < 0.05$) are indicated in **bold**. Corresponding pairwise tests for the interaction term (dataset x increment widths) are also shown.

a)

	Numerator df	Denominator df	Pseudo-*F*	P	Unique permutations
Fixed effects					
Datasets:					
GCRL vs SEAMAP	1	1369	11.783	**0.001**	996
Increments width (0-9)	9	1369	915.380	**0.001**	996
Dataset x Increment width	9	1369	14.136	**0.001**	999
Pairwise	Increment	Denominator df	t	P	Unique permutations
Dataset x Increment	0	171	7.855	**0.001**	969
	1	170	9.247	**0.001**	886
	2	214	6.915	**0.001**	924
	3	209	4.155	**0.001**	948
	4	186	0.39	0.706	962
	5	151	0.692	0.483	960
	6	99	0.888	0.373	942
	7	80	0.337	0.728	898
	8	52	1.924	0.066	321
	9	37	0.559	0.605	452

b)

	Numerator df	Denominator df	Pseudo-*F*	P	Unique permutations
Fixed effects					
Datasets:					
GOM vs Balearic Sea	1	3723	937.89	**0.001**	997
Increment width (1-11)	10	3723	491.71	**0.001**	999
Dataset x Increment width	10	3723	76.679	**0.001**	996

Pairwise	Increment	Denominator df	t	P	Unique permutations
Dataset x Increment width	1	570	0.33712	0.736	995
	2	599	1.1359	0.25	996
	3	575	3.3883	**0.004**	997
	4	537	2.6488	**0.005**	996
	5	460	5.764	**0.001**	994
	6	337	6.1761	**0.001**	992
	7	252	7.3863	**0.001**	993
	8	177	8.4558	**0.001**	977
	9	120	8.8374	**0.001**	985
	10	61	7.3829	**0.001**	829
	11	35	11.086	**0.001**	683